3-D Electron Optics Simulation Method for Cathode Ray Tubes

doi: 10.1109/20.43983

3-D ELECTRON OPTICS SIMULATION METHOD FOR CATHODE RAY TUBES

Y. Ose, T. Takagi, H. Sano and K. Miki
Energy Research Laboratory, Hitachi, Ltd.
1168 Moriyama-cho, Hitachi-shi, Ibaraki-ken, 316 (JAPAN)

A numerical simulation method for 3-D electron optics in an electromagnetic field is described. The method features the following: (1) electric field analysis by a boundary-fitted coordinate transformation method in conjunction with a domain decomposition and overlapping technique; (2) consideration of the space charge effect due to electron beam in a self-consistent electric field; (3) magnetic field analysis based on a current sheet method and a boundary element method; and (4) interactive geometric modelling and numerical grid generation based on the same method as (1). The method was applied to electron optics simulation for an electron gun of a cathode ray tube with a typical deflection yoke. The results of comparison between computed and measured screen spot profiles verified the method and demonstrated its capabilities.

Introduction

Spherical aberration in the main lens and deflection aberration in the deflection region deteriorate the resolution of a cathode ray tube (CRT). In order to reduce spherical aberration, it is effective to increase the lens diameter and to decrease the beam-to-lens diameter ratio. Because the main lens diameter is restricted by the inner diameter of neck tube, many CRTs now incorporate non-cylindrical electron guns to allow for larger lenses. An accurate simulation of the electron beam focus characteristics in these electron guns requires a 3-D analysis method.

There are several approaches to the electric field analysis for electron optics in CRTs. The finite difference method[1] is the most straightforward, but it needs some interpolation between grid points for complicated shapes. The finite element method[2], on the other hand, has geometrical advantages for matching complicated boundaries, but it may require considerable experience and time to divide the domain into finite elements without using some preprocessors. The boundary element method[3] can overcome this problem by calculating unknown variables and its derivatives only on the boundary, thus making generation of the mesh division easier, but treatment of the space charge effect caused by the electron beam is difficult. We have already proposed an approach to electric field analysis by using a boundary-fitted coordinate transformation method. This was based on an automated numerical generation of a curvilinear coordinate system having a coordinate line coincident with each boundary of an arbitrarily shaped domain.

To provide dynamic convergence, the magnetic deflection field consists of a pincushon-shaped horizontal deflection field and a barrel-shaped vertical deflection field. In order to evaluate the beam spot distortion, raster distortion and misconvergence due to those fields, a 3-D analysis method is also required. Early deflection magnetic field analysis was limited to rotationally symmetric yokes and winding coils[4]. These days nonrotationally symmetric deflection yokes and winding coils are expected. We extended the current sheet method to allow treatment of nonrotationally symmetric shaped winding coils and adopted a boundary element method which can give the correct magnetic field in an open, homogeneous space.

This paper presents a solution scheme for electron optics simulation in a self-consistent electric field with a magnetic deflection field. An interactive geometric modelling and grid generation method based on the domain decomposition and overlapping technique are also described, followed by results of some applications to electron optics simulation for CRTs.

Description of Method

Basic Equations

A Poisson's equation governs the steady-state, self-consistent electric field for the electrode voltage and space charge caused by the electron beam,

$$\nabla\cdot(\varepsilon_0\nabla\phi)=-\rho \tag{1}$$

where ϕ is the electric potential, ρ is the distributed space charge density, and ε_0 is the dielectric constant of free space.

Child-Langmuir's law gives cathode current density as follows,

$$j=\frac{4\varepsilon_0}{9}\left(\frac{2e}{m}\right)^{1/2}\frac{\phi_d^{3/2}}{d^2} \tag{2}$$

where e and m are the electron charge and mass, and ϕ_d is the calculated potential at a small distance d near the cathode surface.

A beam trajectory of a sample electron which carries current emitted from an area of the mesh-divided cathode is the solution of the equation of motion:

$$m\ddot{\mathbf{r}}=-e(\mathbf{E}+\mathbf{v}\times\mathbf{B}) \tag{3}$$

where $\mathbf{E}$ is the electric field, $\mathbf{B}$ is the magnetic flux density and $\mathbf{v}$ is the electron velocity.

The governing equation for the static magnetic field free from current are expressed using the magnetic scalar potential Ψ as follows,

$$\mathbf{H}=-\nabla\Psi,\qquad \nabla^2\Psi=0 \tag{4}$$

where $\mathbf{H}$ is the magnetic field intensity.

The calculation flow in the electron optics

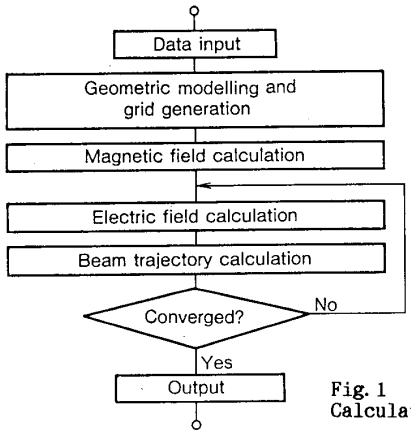

Fig. 1 Calculation flow

0018-9464/88/0100-0552$01.00©1988 IEEE

simulation is illustrated in Fig. 1. After the grid generation, the static magnetic field generated by deflection yokes and winding coils is calculated based on eq. (4). Solutions of eqs. (1)-(3) are repeated until the electric field becomes self-consistent.

Grid Generation

Boundary-Fitted Coordinate Transformation Method: The grid generation technique used in the present study is based on the boundary-fitted coordinate transformation method developed by Mastin and Thompson[5]. The transformation from the physical space (x, y, z) to the transformed space (ξ, η, ζ) is shown in Fig. 2. The 3-D grid is generated by solving the following partial differential equations with Dirichret boundary conditions.

$$\alpha_{11}\mathbf{r}_{\xi\xi}+\alpha_{22}\mathbf{r}_{\eta\eta}+\alpha_{33}\mathbf{r}_{\zeta\zeta}+2\alpha_{12}\mathbf{r}_{\xi\eta}+2\alpha_{13}\mathbf{r}_{\xi\zeta}+2\alpha_{23}\mathbf{r}_{\eta\zeta}+J^2(P\mathbf{r}_{\xi}+Q\mathbf{r}_{\eta}+R\mathbf{r}_{\zeta})=0 \quad (5)$$

where $\mathbf{r}$ is the vector denoting (x, y, z), $\mathbf{r}_{\xi\xi}=\partial^2\mathbf{r}/\partial\xi^2$, $\mathbf{r}_{\xi}=\partial\mathbf{r}/\partial\xi$, etc., and α_{ij} and J are the transformation coefficient and Jacobian respectively. The functions P, Q and R may be chosen to concentrate the grid as desired.

Domain Decomposition and Overlapping Technique: This technique[6] is a variant of the well-known Schwarz alternating procedure. A decomposition of the 3-D domain into subdomains is used and each subdomain has six curved or plane surfaces. Each subdomain grid is generated independently by the boundary-fitted coordinate transformation method. To ensure the composite grid remains both continuous and smooth across the boundaries, an overlap of two grid surfaces is adopted between any two adjacent hexahedrons. The inner grid coordinates are calculated using the Dirichret boundary conditions on six surfaces of a hexahedron, and the calculated coordinates on the overlapping surfaces are transformed to the surface of a neighboring one. This procedure is repeated for all hexahedrons until the convergence requirement is met for all grid points. This technique is also used for potential and beam calculations.

Interactive geometric modelling and grid generation: The present method has the functions of geometric modelling and grid generation for 2-D and 3-D geometries. Using arbitrary curve and curved surface representations, it can treat an arbitrarily shaped geometry. The 2-D geometry is expressed by wire-frames such as lines, circles and splines. The 3-D geometry is expressed by a boundary-representation technique [7]. The global curved surface is formed by patching small portions of curved surfaces together. The 2-D and 3-D grids are generated by using the domain decomposition and overlapping technique in conjunction with the boundary-fitted coordinate transformation method.

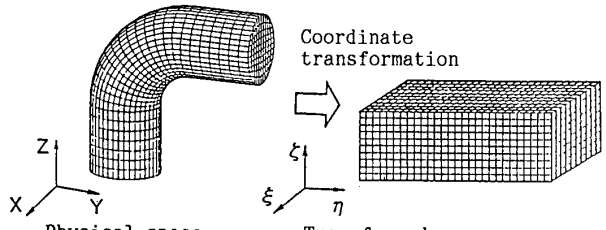

Fig. 2 Boundary-fitted coordinate transformation

Electric Field Analysis

The Poisson's equation (1) is transformed into the curvilinear coordinate system (ξ, η, ζ) and solved. The integral form of eq. (1)

$$\iiint\nabla\cdot(\varepsilon_0\nabla\phi)\,dV=\iiint(-\rho)\,dV \quad (6)$$

is discretized in this coordinate system. The integral form agrees with the so-called fully conservative form and is known to give more accurate solutions in a curvilinear coordinate system. The left-hand side of eq. (6) can be written using Gauss's divergence theorem and discretized as follows,

$$\begin{aligned}&\iint(\varepsilon_0\nabla\phi)\cdot n\,dS\\&=[(\varepsilon_0\nabla\phi)\cdot n^{(\xi)}\Delta S^{(\xi)}]_{\xi+}-[(\varepsilon_0\nabla\phi)\cdot n^{(\xi)}\Delta S^{(\xi)}]_{\xi-}\\&+[(\varepsilon_0\nabla\phi)\cdot n^{(\eta)}\Delta S^{(\eta)}]_{\eta+}-[(\varepsilon_0\nabla\phi)\cdot n^{(\eta)}\Delta S^{(\eta)}]_{\eta-}\\&+[(\varepsilon_0\nabla\phi)\cdot n^{(\zeta)}\Delta S^{(\zeta)}]_{\zeta+}-[(\varepsilon_0\nabla\phi)\cdot n^{(\zeta)}\Delta S^{(\zeta)}]_{\zeta-}\end{aligned} \quad (7)$$

where the subscripts $\xi+$, $\xi-$, etc. indicate evaluation on the surfaces of the volume element shown in Fig. 3. n and ΔS are the normal vectors and the area elements of these surfaces. A generalized boundary condition is given as

$$c_1\phi+c_2\,n\cdot\nabla\phi=c_3 \quad (8)$$

where c_1, c_2 and c_3 are parameters. Boundary conditions are also transformed and discretized in the transformed space.

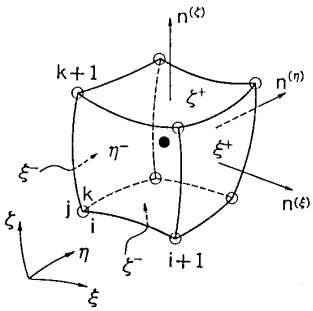

Fig. 3 Calculation cell defined by curvilinear coordinate in physical space

Magnetic Field Analysis

Current Sheet Method: Assuming the current within thin sheets (current sheets), the effect of the current on the magnetic field[8] can be represented by a potential gap Ψg between the upper and lower surfaces as shown in Fig. 4.

$$\Psi g\equiv\Psi_1-\Psi_2=\int_0^t(\mathbf{n}\times\mathbf{i})\,dt \quad (9)$$

where the subscripts 1 and 2 indicate values on the upper and lower sides respectively, $\mathbf{i}$ and $\mathbf{n}$ are the current and normal vectors respectively and t is the distance along the curve L.

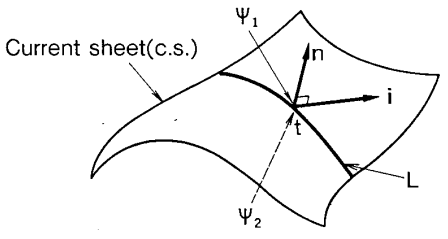

Fig. 4 Current sheet method

Boundary Element Method: Fig. 5 shows a cross-sectional view of a core and a current sheet. The potential $\Psi(P)$ inside the core and $\Psi'(P')$ outside it can be expressed by the following integral equations,

$$\Psi(P) = -\int_{core} [\Psi(Q)\frac{\partial G}{\partial n}(P,Q) - \frac{\partial \Psi}{\partial n}(Q)\,G(P,Q)]\,d\Gamma \quad (10)$$

$$\Psi'(P') = \int_{core} [\Psi'(Q)\frac{\partial G}{\partial n}(P',Q) - \frac{\partial \Psi'}{\partial n}(Q)\,G(P',Q)]\,d\Gamma + \int_{c.s.} \Psi_g(S)\frac{\partial G}{\partial n}(P',S)\,d\Gamma \quad (11)$$

where $\Psi(Q)$ and $\partial\Psi/\partial n(Q)$ are the potential and the normal derivative on the core respectively, and G is Green's function. $\int_{core} d\Gamma$ and $\int_{c.s.} d\Gamma$ indicate the surface integrations on the core and current sheet respectively. Solving these equations by using the boundary element method, the magnetic field intensity $\mathbf{H}$ is computed as follows,

$$\mathbf{H} = \int_{core} [\Psi(\nabla\frac{\partial G}{\partial n}) - \frac{\partial \Psi}{\partial n}(\nabla G)]\,d\Gamma - \int_{c.s.} \Psi_g(\nabla\frac{\partial G}{\partial n})\,d\Gamma. \quad (12)$$

When the current sheet locates on the core, the following equation is used in order to avoid the singularity of Green's function.

$$\mathbf{H} = \int_{core} [(\Psi - \Psi_g)(\nabla\frac{\partial G}{\partial n}) - \frac{\partial \Psi}{\partial n}(\nabla G)]\,d\Gamma \quad (13)$$

Numerical Results and Discussion

Electron Beam Analysis in an Electric Field

The method was applied to the electron optics simulation of an electron gun with six electrodes. Fig. 6 explains the process of geometric modelling and grid generation and shows some calculated results. A cross-section of the electrode geometry is shown in Fig. 6(a). The 2-D wire-frame model in Fig. 6(b) was created by connecting the input points (asterisks) using lines and curves. After the domain was divided into 27 subdomains, the initial grid was generated by linear interpolation in each subdomain (Fig. 6(c)). Then the 2-D optimized grid was calculated using the grid generation method (Fig. 6(d)). The 3D wire-frame model was obtained by sweeping the 2-D model along the guide curves. The 3-D optimized grid was finally obtained by the grid generation method (Fig. 6(e)). The total number of generated grid points was about 60,000. Fig. 6(f) shows the potential distribution and beam trajectories, which are solved assuming constant field in a cell. The space charge caused by a beam trajectory in a cell is distributed to the surrounding 8 grid points. Beam spot size at the screen center was obtained by further calculation in the deflection region, considering the space charge effect. The calculated values agreed with measured values within 10%.

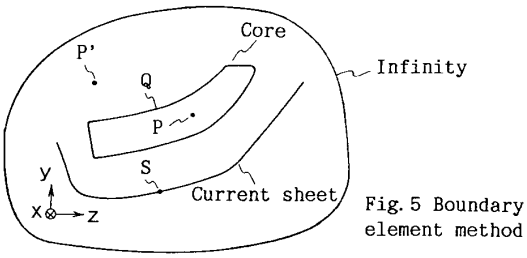

Fig. 5 Boundary element method

Electron Beam Analysis in a Magnetic Field

Fig. 7 shows the surface grid generated on a 110° deflection yoke consisting of saddle and toroidal coils and a core. There were 396 and 252 grid points on the saddle coil and the core, respectively. Figs. 8 and 9 show the distribution of the magnetic field caused by the saddle coil and toroidal coil respectively, while changing the specific permeability μ_r from 80 to 350.

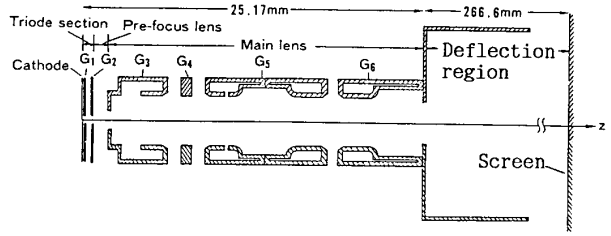

(a) Electrode geometry of CRT

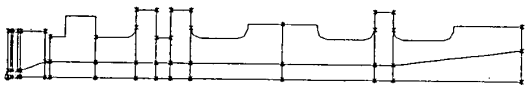

(b) Input points and decomposed domain

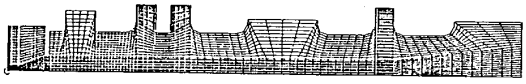

(c) 2—D initial grid

(d) 2—D generated grid

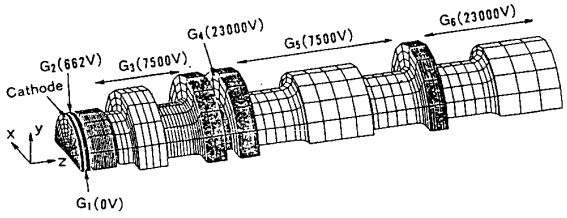

(e) 3—D optimized grid

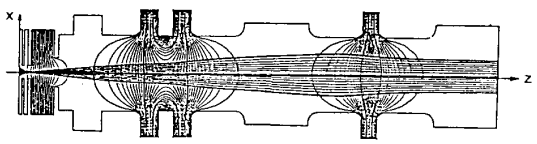

(f) Potential distribution and beam trajectory

Fig. 6 Electron optics simulation for electron gun

Calculated values agreed within 5% with measured ones at μ_r=80 for the saddle coil and at μ_r=200 for the toroidal coil. The difference in specific permeability was due to the fact that the saddle coil produced the stronger magnetic field than the toroidal coil.

Electron beam trajectories in the deflection region were calculated. The initial condition of the electron beam was provided from the electron

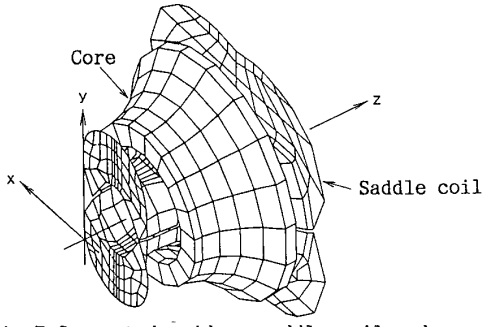

Fig. 7 Generated grid on saddle coil and core

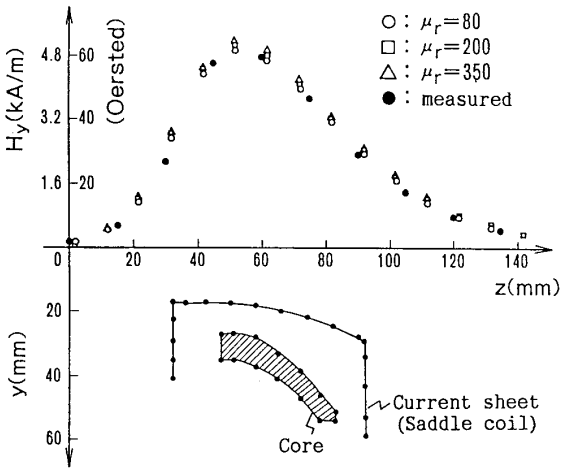

Fig. 8 Distribution of the magnetic field caused by saddle coil

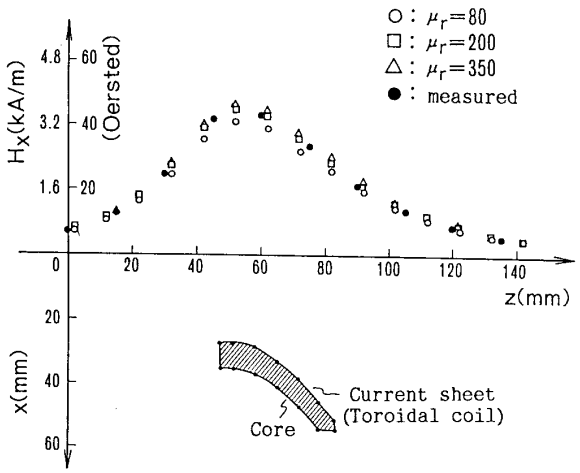

Fig. 9 Distribution of the magnetic field caused by toroidal coil

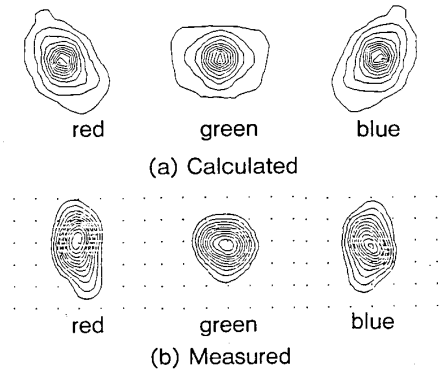

Fig. 10 Beam spot profiles on the screen top

beam analysis described above. Fig. 10 compares between the calculated and measured contours of the beam current density at the screen top. Calculated profiles of the low current density region (halo) qualitatively agreed with measured ones.

Conclusions

A method of 3-D electron optics simulation has been developed. The electric field analysis was based on a boundary-fitted coordinate transformation method with a technique of decomposing the analysis domain into several subdomains. The magnetic field analysis was based on a current sheet and a boundary element method.

The present method was applied to electron beam analysis of a CRT. Calculated beam spot size at the screen center agreed with measured values within 10%. Beam spot profiles at the screen top agreed with measured ones where the analyzed magnetic field caused by a deflection yoke agreed with measured values within 5%.

References

[1] M. van den Broek, "Simulation of 3D Electron Beams with a Fitting Technique", Optik vol. 71, no. 1, 1985, pp. 27-35

[2] D. M. MacGregor, "Computer-Aided Design of Color Picture Tubes with a Three-Dimentional Model", IEEE Trans. Electron Devices, vol. ED-33, no. 8, 1980, pp. 1098-1106

[3] K. Hosokoshi, et al., "Improved OLF In-Line Gun System", Japan Display, 1983, pp. 272-275

[4] E. Thone Hall, "Combination Boundary Integral and Finite Difference Method for Calculation of Yoke Magnetic Fields", SID 85 Digest, 1985, pp. 170-173

[5] C. W. Mastin and J. F. Thompson, "Transformation of Three-Dimentional Regions onto Rectangular Regions by Elliptic Systems", Numerische Mathematik, vol. 29, 1978, pp. 397-407

[6] K. Miki, et al., "Numerical Solution of Poisson's Equation with Arbitrarily Shaped Boundaries Using a Domain Decomposition and Overlapping Technique", J. Comput. Physics, vol. 67, no. 2, 1986

[7] A. Bear, et al., "Geometric Modelling: A Survey", Computer Aided Design, vol. 11, no. 5, 1979

[8] H. Sano, et al., "Three-Dimensional Analysis by a Current Sheet Method for Static Magmetic Field", Elec. Eng. in Japan (to be published)